SEMARAK ILMU PUBLISHING

Journal of Advanced Research in Applied Mechanics

Journal homepage:
https://semarakilmu.com.my/journals/index.php/appl_mech/index
ISSN: 2289-7895

Response Surface Methodology of the Unsteady Axisymmetric Magnetic Hybrid Nanofluid Flow Subject to a Shrinking Disk

Najiyah Safwa Khashi'ie[1,3,*], Khairum Bin Hamzah[2,3], Iskandar Waini[2,3], Nurul Amira Zainal[1,3], Sayed Kushairi Sayed Nordin[1,3], Abdul Rahman Mohd Kasim[4], IoanPop[5]

[1] Fakulti Teknologi dan Kejuruteraan Mekanikal, Universiti Teknikal Malaysia Melaka, Hang Tuah Jaya, 76100 Durian Tunggal, Melaka, Malaysia
[2] Fakulti Teknologi dan Kejuruteraan Industri dan Pembuatan, Universiti Teknikal Malaysia Melaka, Hang Tuah Jaya, 76100 Durian Tunggal, Melaka, Malaysia
[3] Forecasting and Engineering Technology Analysis (FETA) Research Group, Universiti Teknikal Malaysia Melaka,76100 Durian Tunggal, Malaysia
[4] Pusat Sains Matematik, Universiti Malaysia Pahang Al-Sultan Abdullah, Lebuh Persiaran Tun Khalil Yaakob, 26300 Kuantan, Pahang, Malaysia
[5] Department of Mathematics, Babeş-Bolyai University, R-400084 Cluj-Napoca, Romania

ARTICLE INFO

Article history:
Received 21 August 2023
Received in revised form 23 October 2023
Accepted 9 November 2023
Available online 5 January 2024

Keywords:
Hybrid nanofluid; response surface analysis; shrinking disk; unsteady flow

ABSTRACT

This study examines the unsteady Fe_3O_4-$CoFe_2O_4/H_2O$ flow over a shrinking disk using both procedures (numerical and statistical). The respective boundary layer model is first transformed into a set of ODEs (ordinary differential equations) using the similarity transformations, and then solved numerically using the bvp4c solver. The duality of solutions is presented within specific use of the parameters such as magnetic field, suction strength and volumetric concentration of hybrid nanoparticles. From the numerical results, the velocity profile increases as the suction and magnetic parameters slightly increase. However, the temperature profile shows a reverse trend as compared to the velocity profile. Meanwhile, the justification of present physical factors (magnetic parameter, suction parameter) whether they are significant or not on the development of responses is tested using the model in Minitab. In addition, the generated response equation is also beneficial in predicting the flow and thermal distributions of this working fluid for other values of the emerging parameters.

1. Introduction

Numerous researchers have conducted research on boundary layer flow motivated by its potential applications such as automotive, aircraft airfoil design and ship friction drag. The initial investigations focused on the viscous fluid flow over stretching/shrinking sheet, with Crane [1] and Miklavčič and Wang [2] being the pioneers in this field. A stretching sheet typically enables a viable boundary layer solution as it induces suction towards the surface, facilitating the flow. Conversely, Miklavčič and Wang [2] highlighted the necessity of a suction effect to maintain the fluid movement against the shrinking sheet, which led to the discovery of two solutions with appropriate suction. Subsequently, Wang [3] observed the occurrence of two solutions in stagnation point flow towards

* *Corresponding author.*
E-mail address: najiyah@utem.edu.my

https://doi.org/10.37934/aram.112.1.137148

a shrinking sheet, without the need for a suction parameter in cases involving shrinking, as the vorticity could be confined within the boundary layer by the free stream flow. This led to further investigations involving different surface types (e.g., disk, wedge) and various shrinking/ stretching velocity (nonlinear, linear). The pursuit of optimal heat transfer performance in technological and industrial applications has spurred the recent invention and exploration of hybrid nanofluids (see Sheremet *et al.,* [4-6], Babazadeh *et al.,* [7], Zhang *et al.,* [8], Devi and Devi [9,10], Bakar *et al.,* [11], Takabi and Salehi [12] and several research papers [13-17]). Waini *et al.,* [18,19] identified two solutions in both cases (shrinking and rigid surfaces) by considering the unsteadiness decelerating parameter. Conversely, Zainal *et al.,* [20, 21] demonstrated that the accelerating parameter also led to dual solutions. Khashi'ie *et al.,* [22] discovered that the incorporation of the decelerating parameter could positively affect the thermal rate.

In addition to numerical interpretations, employing experimental design in research offers numerous advantages, especially when dealing with multiple factors or parameters and their corresponding outcomes. One commonly used design type is Response Surface Methodology (RSM), which is utilized for analyzing and modeling processes where the response is influenced by various variables. The methodology aims to determine the interaction effects among independent variables. To ascertain the statistical significance of the experiment's variables, an analysis of variance/ANOVA is conducted. Mehmood *et al.,* [23] discussed the use of ANOVA and RSM for the rotating disk case. Furthermore, RSM and statistical data analysis have been applied to various fluid flow problems, as demonstrated in these studies [24-26].

Therefore, our primary objectives are twofold. Firstly, we intend to produce all viable numerical solutions with the current model. Second, we propose to analyze the data using RSM and statistical analysis. In order to accomplish these goals, the governing model is initially transformed via similarity transformation into a set of ODEs. ANOVA is carried out utilizing the Minitab software's fit general linear model. The central composite design in RSM is used to choose the data for analysis. By considering the physical factors, a fitted model for the responses is produced based on the statistical data analysis. These equations can be applied in real-world situations and in further studies of unsteady flow brought on by a shrinking disk. The major components that contribute to the formation of the response are further identified by statistical data analysis. Since no other study of this kind has been done, we think that the novelty and importance of our work are justified. We are certain that our study will draw a large audience of readers and scholars interested in advancing this research issue because it contributes to the exploration of both statistical data analysis and numerical solutions.

2. Mathematical Formulation

The present investigation highlights the unsteady magnetic nanofluid Fe_3O_4-$CoFe_2O_4$/H_2O flow over a shrinking disk, as depicted in Figure 1. The fluid motion is influenced by a shrinking disk with velocity $u_w(r,t) = cr/\sqrt{1-\alpha t}$. Several assumptions are considered in this analysis:

i. The wall temperature is denoted by T_w, while T_∞ represents the ambient temperature.
ii. $B^* = B_0/\sqrt{1-ct}$ is the magnetic field strength which directed perpendicular to the sheet with constant B_0.
iii. $v_w(r,t) = -2\sqrt{\frac{c\nu_f}{1-\alpha t}}S$ denotes the permeable disk's mass flux velocity with $S>0$ indicating suction and $S<0$ indicating injection.

iv. The model does not account for the impact of sedimentation/aggregation. This assumption allows for a simplified analysis and interpretation of the numerical data, focusing on other relevant factors or phenomena that influence the hybrid nanofluid's performance.

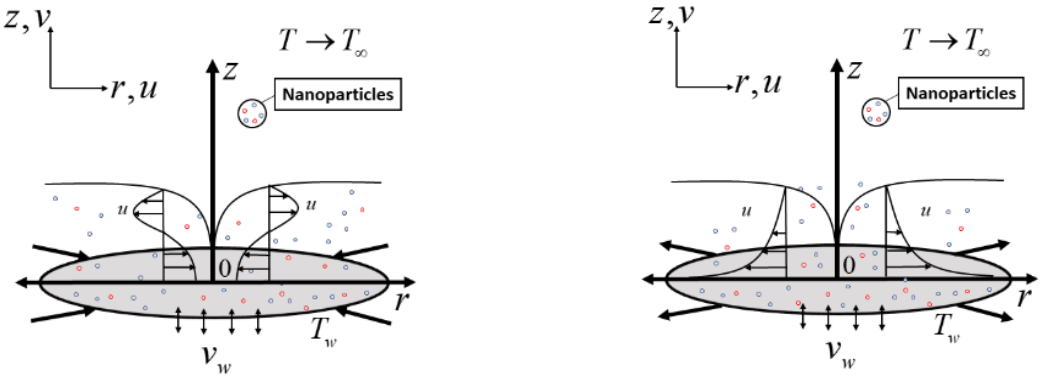

Fig. 1. The physical model for (a) shrinking disk and (b) stretching disk

Hence, the governing model is:

$$\frac{\partial}{\partial r}(ru)+\frac{\partial}{\partial z}(rw)=0, \tag{1}$$

$$\frac{\partial u}{\partial t}+u\frac{\partial u}{\partial r}+w\frac{\partial u}{\partial z}=\frac{\mu_{hnf}}{\rho_{hnf}}\frac{\partial^2 u}{\partial z^2}-\frac{\sigma_{hnf}}{\rho_{hnf}}B^{*2}u, \tag{2}$$

$$\frac{\partial T}{\partial t}+u\frac{\partial T}{\partial r}+w\frac{\partial T}{\partial z}=\frac{k_{hnf}}{\left(\rho C_p\right)_{hnf}}\frac{\partial^2 T}{\partial z^2}, \tag{3}$$

subject to

$$\left.\begin{aligned} t\geq 0:\ u=\lambda u_w,\ v=v_w,\quad T=T_w \quad \text{at}\quad z=0 \\ u\to 0,\quad T\to T_\infty \quad \text{as}\quad z\to\infty \end{aligned}\right\}. \tag{4}$$

The velocities in these equations are u and v while T denotes the fluid temperature. The stretching/shrinking parameter is represented by λ such that $\lambda>0$ and $\lambda<0$ are for the stretched and shrunk surfaces, respectively, whereas the static sheet is indicated by $\lambda=0$. The following similarity transformation is used to simplify the system of Eq. (2)-(6)

$$\psi=-r^2\sqrt{\frac{c\nu_f}{1-\alpha t}}f(\eta),\quad \theta(\eta)=\frac{T-T_\infty}{T_w-T_\infty},\quad \eta=z\sqrt{\frac{c}{\nu_f(1-\alpha t)}}. \tag{5}$$

Here, ψ denotes the stream function with $u=-\frac{1}{r}\frac{\partial\psi}{\partial z}=\frac{cr}{1-\alpha t}f'(\eta)$ and $v=\frac{1}{r}\frac{\partial\psi}{\partial r}=-2\sqrt{\frac{c\nu_f}{1-\alpha t}}f(\eta)$ which fulfilled Eq. (1). Upon the similarity transformation, the governing equations in Eq. (2) and Eq. (3) with boundary condition Eq. (5) are reduced to:

$$\frac{\mu_{hnf}/\mu_f}{\rho_{hnf}/\rho_{hnf}}f'''+2ff''-f'^2-\frac{\sigma_{hnf}/\sigma_f}{\rho_{hnf}/\rho_{hnf}}Mf'-\gamma\left(f'+\frac{\eta}{2}f''\right)=0, \tag{6}$$

$$\frac{1}{\Pr}\frac{k_{hnf}/k_f}{\left(\rho C_p\right)_{hnf}/\left(\rho C_p\right)_f}\theta''-\gamma\frac{\eta}{2}\theta'+2f\theta'=0, \tag{7}$$

$$\begin{aligned} &f(0)=S, \quad f'(0)=\lambda, \quad \theta(0)=1 \\ &f'(\eta)\to 0, \quad \theta(\eta)\to 0 \quad \text{as} \quad \eta\to\infty \end{aligned} \tag{8}$$

The parameters appear in Eqs. (6)-(8) are defined as Prandtl number $\Pr=(\mu C_p)_f/k_f$, the magnetic parameter $M=\sigma_f B_0^2/c\rho_f$ and unsteadiness parameter $\gamma=\alpha/c$ while other parameters have been specified earlier. Table 1 displays the experimentally validated correlations of properties for hybrid nanofluids, as presented by Takabi and Salehi [12]. These correlations are established based on physical assumptions and are applicable for both experimental and numerical investigations. They provide a means to estimate various properties of hybrid nanofluids using the given inputs. To facilitate computational analysis, Table 2 lists the specific properties that are employed in the calculations [27]. These properties serve as inputs for the modeling and simulation of hybrid nanofluid behavior.

Table 1
Correlations of hybrid nanofluid

Properties	Hybrid Nanofluid
Dynamic Viscocity	$\mu_{hnf}=\frac{\mu_f}{\left(1-\phi_{hnf}\right)^{2.5}}, \quad \phi_{hnf}=\phi_1+\phi_2$
Heat Capacity	$\left(\rho C_p\right)_{hnf}=\phi_1\left(\rho C_p\right)_{s1}+\phi_2\left(\rho C_p\right)_{s2}+\left(1-\phi_{hnf}\right)\left(\rho C_p\right)_f$
Electrical Conductivity	$\sigma_{hnf}=\left[\frac{\left(\frac{\phi_1\sigma_1+\phi_2\sigma_2}{\phi_{hnf}}\right)-2\phi_{hnf}\sigma_f+2\left(\phi_1\sigma_1+\phi_2\sigma_2\right)+2\sigma_f}{\left(\frac{\phi_1\sigma_1+\phi_2\sigma_2}{\phi_{hnf}}\right)+\phi_{hnf}\sigma_f-\left(\phi_1\sigma_1+\phi_2\sigma_2\right)+2\sigma_f}\right]\sigma_f$
Thermal Conductivity	$k_{hnf}=\left[\frac{\left(\frac{\phi_1k_1+\phi_2k_2}{\phi_{hnf}}\right)-2\phi_{hnf}k_f+2\left(\phi_1k_1+\phi_2k_2\right)+2k_f}{\left(\frac{\phi_1k_1+\phi_2k_2}{\phi_{hnf}}\right)+\phi_{hnf}k_f-\left(\phi_1k_1+\phi_2k_2\right)+2k_f}\right]k_f$
Density	$\rho_{hnf}=\phi_1\rho_{s1}+\phi_2\rho_{s2}+\left(1-\phi_{hnf}\right)\rho_f$

Table 2
Thermophysical properties for magnetite, cobalt ferrite and water

Thermophysical Properties	Fe_3O_4	H_2O	$CoFe_2O_4$
ρ (kg/m^3)	5180	997.1	4908
k (W/mK)	9.8	0.6130	3.6
σ (S/m)	0.74 x 10^6	0.05	1.1 x 10^7
C_p(J/kgK)	670	4179	700

The physical quantities of interest are the skin friction coefficient and thermal transfer rate which are respectively given as:

$$0.5\,\mathrm{Re}_r^{1/2}\,C_f = \frac{\mu_{hnf}}{\mu_f} f''(0), \qquad \mathrm{Re}_r^{-1/2}\,Nu_r = -\frac{k_{hnf}}{k_f}\theta'(0) \tag{9}$$

where $\mathrm{Re}_x = ru_w/\nu_f$ denotes the local Reynolds number.

3. Results and Discussion

In this section, the bvp4c is used to compute the similarity solutions for Eq. (6) and Eq. (7) as well as its boundary condition Eq. (8). The performances of Fe_3O_4-$CoFe_2O_4$/H_2O are investigated for specific conditions: $\mathrm{Pr} = 6.2$, $\lambda = \gamma = -2$, $0 \le M \le 0.5$, $3 \le S \le 4$ and $0.01 \le \phi_{hnf} \le 0.03$. The corresponding Figure 2 and Figure 3, illustrate the effects of magnetic and suction parameters on the profiles of temperature and velocity. It is worth noting that the presence of multiple solutions is observed within the given parameters. Usually, the first solution which fulfilled the boundary conditions is denoted as the physical stable solution. Hence, for the RSM part, only the first solution is considered. It is apparent that both solutions asymptotically fulfilled the far field condition which verified the accuracy of the present solution.

The impact of magnetic parameter is presented in Figures 2(a) and 2(b) respectively for the velocity and temperature. The velocity enhances with the addition of magnetic parameter whereas the temperature is reduced. Meanwhile, the second solution shows the opposite trend. Figures 3(a) and 3(b) demonstrate the impact of suction on the hybrid nanofluid profiles. Both the momentum and thermal boundary layers' thicknesses are reduced by the suction parameter. As a result, it improves the velocity profile while decreasing the temperature profile. This effect can be attributed to suction's ability to reduce the momentum boundary layer thickness, leading to improved flow (increased velocity). Additionally, suction induces the movement of heated fluid particles towards the wall, resulting in increased heat transfer and a decrease in temperature.

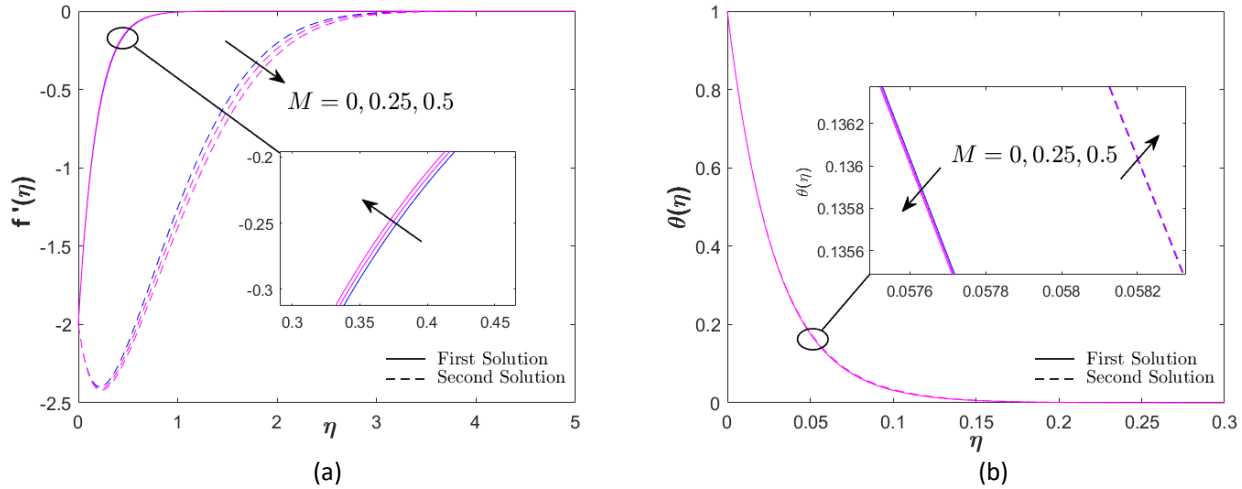

(a) (b)

Fig. 2. (a) Velocity and (b) temperature profiles when $\Pr = 6.2$, $\lambda = \gamma = -2$, $S = 3$ and $\phi_{hnf} = 0.02$

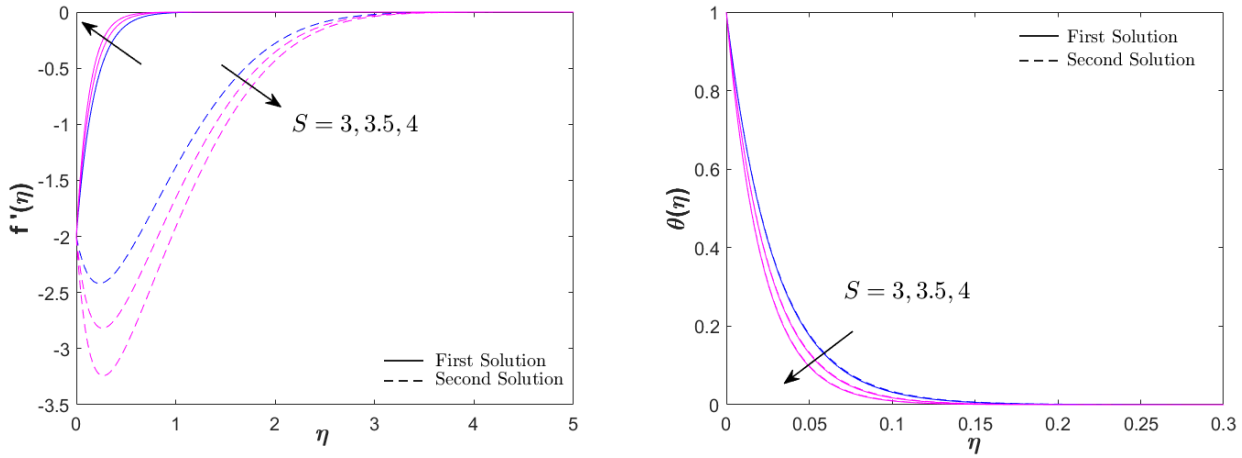

(a) (b)

Fig. 3. (a) Velocity and (b) temperature profiles when $\Pr = 6.2$, $\lambda = \gamma = -2$, $M = 0.5$ and $\phi_{hnf} = 0.02$

4. Response Surface Methodology (RSM)

The experimental design plays a crucial role in addressing the boundary layer flow problem and analyzing the data. It allows us to determine the influential and beneficial factors that optimize the responses, such as the skin friction coefficient and thermal rate. Statistical data analysis helps to identify the factor that contributes to enhancing the responses. In Table 3, the RSM employing the central composite design is highlighted, which consists of 19 runs for 3 factors. The magnetic parameter, suction, and hybrid nanoparticles concentration are denoted as A, B, and C, respectively. These factors are classified into low (-1), medium (0), and high (+1) levels to represent their magnitudes. The total number of runs for these three factors follows the formula mentioned as $R = C + 2k + 2^k$ whereby C, $2k$ and 2^k denotes the center point, axial point and factorial point, respectively [23]. In this study, the five center points with $k = 3$ are used. Based on Table 3, a general response surface equation (10) can be computed. This equation considers intercept (r_0), linear effects (r_A, r_B, r_C), quadratic effects $(r_{A^2}, r_{B^2}, r_{C^2})$, and interaction effects (r_{AB}, r_{CA}, r_{BC}). Since this study focuses on two responses, two surface equations are considered.

$$y = r_0 + r_{\mathrm{A}}\mathrm{A} + r_{\mathrm{B}}\mathrm{B} + r_{\mathrm{C}}\mathrm{C} + r_{\mathrm{AB}}\mathrm{AB} + r_{\mathrm{CA}}\mathrm{CA} + r_{\mathrm{BC}}\mathrm{BC} + r_{\mathrm{A}^2}\mathrm{A}^2 + r_{\mathrm{B}^2}\mathrm{B}^2 + r_{\mathrm{C}^2}\mathrm{C}^2 + \varepsilon \quad (10)$$

Table 3
RSM for the case of $\mathrm{Pr} = 6.2$ and $\lambda = \gamma = -2$

Runs	Real			Coded			Responses	
	M	S	ϕ_{hnf}	A	B	C	$0.5\mathrm{Re}_r^{1/2} C_f$	$\mathrm{Re}_r^{-1/2} Nu_r$
1	0.25	3.5	0.02	0	0	0	13.9160	42.8810
2	0.5	3	0.03	1	-1	1	12.0612	36.5658
3	0.25	3.5	0.02	0	0	0	13.9160	42.8810
4	0	3.5	0.02	-1	0	0	13.8287	42.8805
5	0.25	3.5	0.02	0	0	0	13.9160	42.8810
6	0	4	0.01	-1	1	-1	13.2917	42.9606
7	0.5	4	0.01	1	1	-1	15.7001	49.1985
8	0.25	3.5	0.01	0	0	-1	13.3778	42.9610
9	0.5	3.5	0.02	1	0	0	14.0022	42.8815
10	0.25	3.5	0.02	0	0	0	13.9160	42.8810
11	0.25	3.5	0.03	0	0	1	14.4531	42.8009
12	0	4	0.03	-1	1	1	16.8004	49.0181
13	0.25	4	0.02	0	1	0	16.2522	49.1083
14	0	3	0.03	-1	-1	1	11.8399	36.5641
15	0.25	3	0.02	0	-1	0	11.5015	36.6355
16	0.25	3.5	0.02	0	0	0	13.9160	42.8810
17	0.5	3	0.01	1	-1	-1	11.1562	36.7068
18	0.5	4	0.03	1	1	1	16.9482	49.0187
19	0	3	0.01	-1	-1	-1	10.9410	36.7052
20	0.25	3.5	0.02	0	0	0	13.9160	42.8810

Table 4 displays the statistical analysis results, analyzing the effects of A, B, and C and their interactions on the skin friction (response 1) and heat transfer rate (response 2). The F-value indicates that the factors A, B, C and the interactions AB, AC and BC provide a significant effect on the $0.5\mathrm{Re}_r^{1/2} C_f$ (p-values < 0.05). Meanwhile, for the $\mathrm{Re}_r^{-1/2} Nu_r$, only factor B as well as the interactions AB, AC and BC are significant to the heat transfer data. The high value of R-squared (R-sq) and R-sq (adj) for the skin friction and heat transfer indicate that both models fit the data well. The fitted models by considering the effects and its interactions are:

$$y_{0.5\mathrm{Re}_r^{1/2} C_f} = 13.9570 + 0.317\mathrm{A} + 2.149\mathrm{B} + 0.764\mathrm{C} + 0.265\,\mathrm{AB} - 0.282\mathrm{AC} + 0.369\mathrm{BC} - 0.104\mathrm{A}^2 - 0.142\mathrm{B}^2 - 0.104\mathrm{C}^2 \quad (11)$$

$$y_{\mathrm{Re}_r^{-1/2} Nu_r} = 42.9940 + 0.624\mathrm{A} + 5.613\mathrm{B} + 0.544\mathrm{C} + 0.779\,\mathrm{AB} - 0.780\mathrm{AC} + 0.770\mathrm{BC} - 0.284\mathrm{A}^2 - 0.293\mathrm{B}^2 - 0.284\mathrm{C}^2 \quad (12)$$

Table 4
Statistical analysis result

Source	DF	Adj SS	Adj MS	F-Value	P-Value
Response 1: Skin friction coefficient					
A	1	1.0024	1.0024	9.41	0.012
B	1	46.1941	46.1941	433.85	0.000
C	1	5.8308	5.8308	54.76	0.000
A*A	1	0.0295	0.0295	0.28	0.610
B*B	1	0.0556	0.0556	0.52	0.486
C*C	1	0.0295	0.0295	0.28	0.610
A*B	1	0.5618	0.5618	5.28	0.044
A*C	1	0.6353	0.6353	5.97	0.035
B*C	1	1.0899	1.0899	10.24	0.010
Error	10	1.0648	0.1065		
Lack-of-Fit	5	1.0648	0.2130	*	*
Pure Error	5	0.0000	0.0000		
Total	19	56.8289			
R-sq	98.13%	R-sq (adj)	96.44%		
Response 2: Heat transfer rate					
A	1	3.897	3.897	4.84	0.052
B	1	315.022	315.022	391.52	0.000
C	1	2.954	2.954	3.67	0.084
A*A	1	0.221	0.221	0.27	0.612
B*B	1	0.235	0.235	0.29	0.600
C*C	1	0.221	0.221	0.27	0.612
A*B	1	4.860	4.860	6.04	0.034
A*C	1	4.863	4.863	6.04	0.034
B*C	1	4.743	4.743	5.89	0.036
Error	10	8.046	0.805		
Lack-of-Fit	5	8.046	1.609	*	*
Pure Error	5	0.0000	0.0000		
Total	19	347.096			
R-sq	97.68%	R-sq (adj)	95.60%		

In addition, the contour plot of the interactions between two factors (A/magnetic parameter, B/suction parameter and C/volumetric concentration of the hybrid nanofluid) for both skin friction coefficient and heat transfer rate is displayed in Figure 4 and Figure 5, respectively.

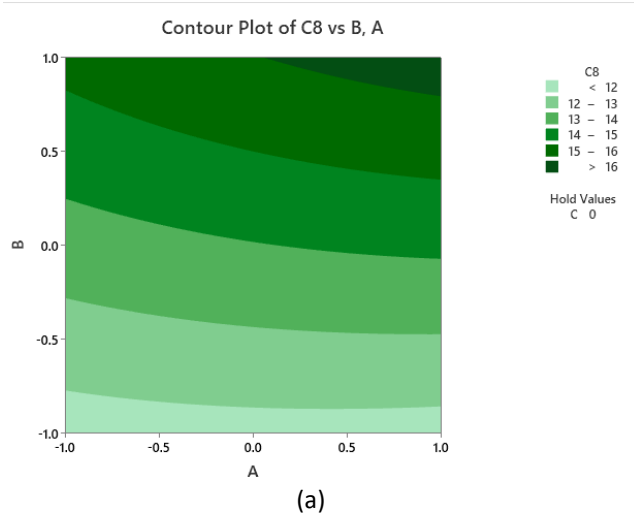

(a)

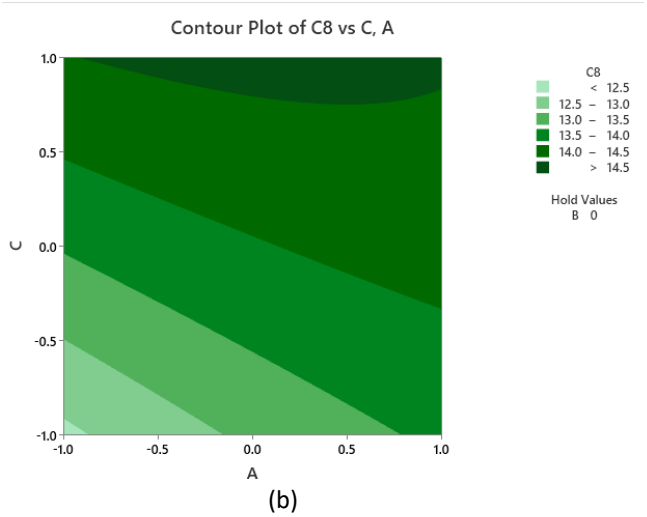

(b)

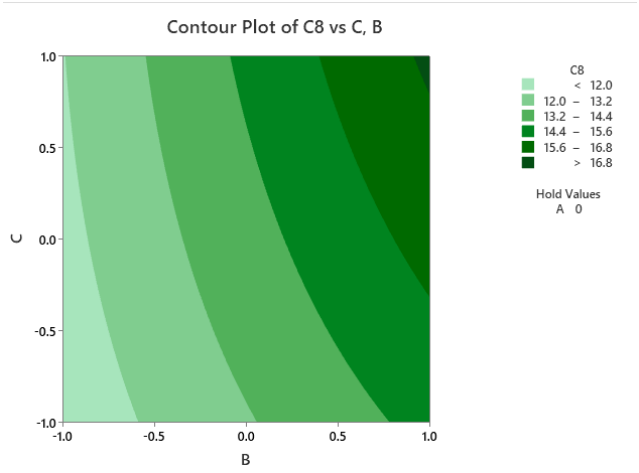

(c)

Fig. 4. Interactions between the parameters (a) B and A, (b) C and A, and (c) C and B for the skin friction coefficient

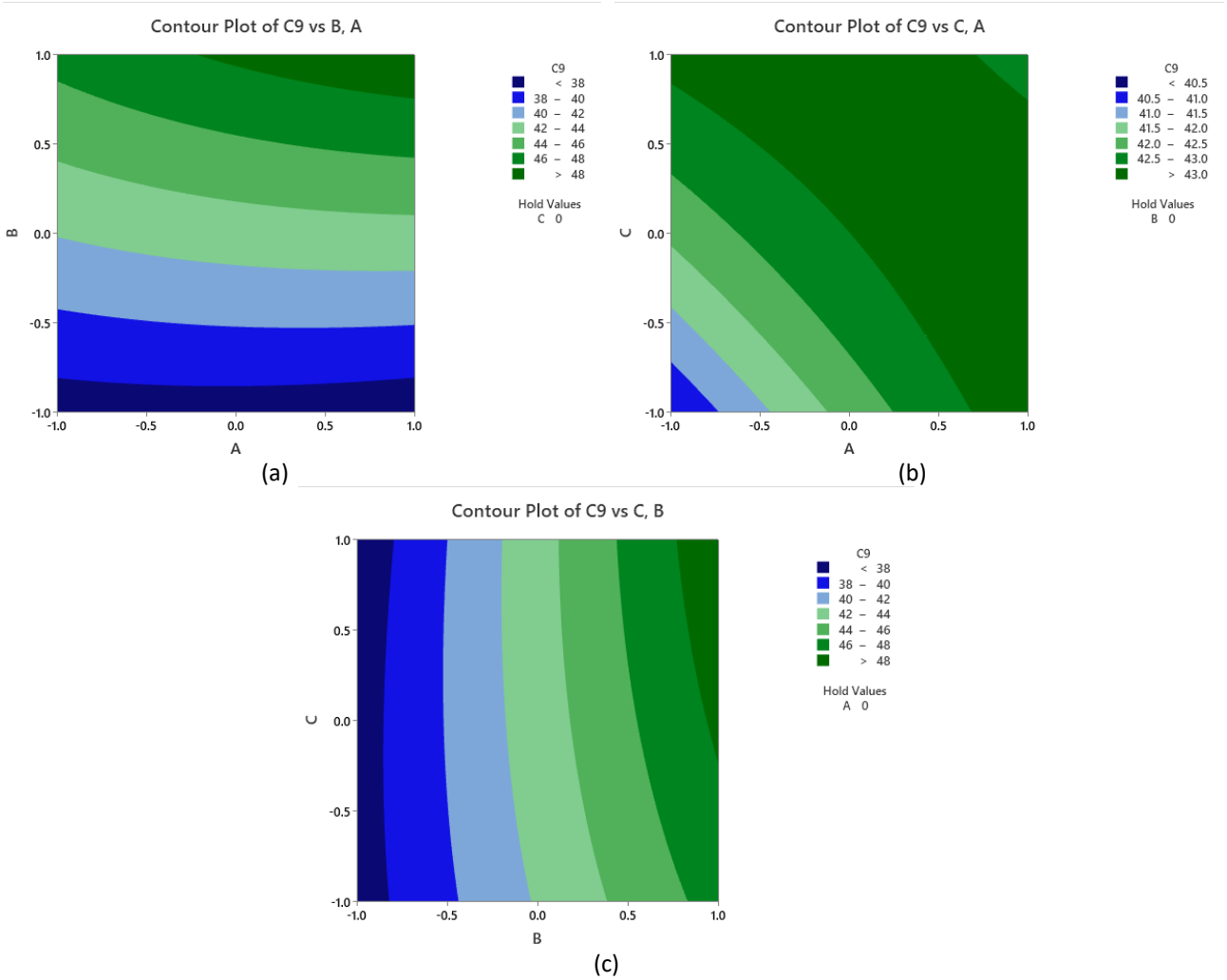

(a) (b)

(c)

Fig. 5. Interactions between the parameters (a) B and A, (b) C and A, and (c) C and B for the heat transfer rate

5. Conclusions

The study focuses on investigating the Fe_3O_4-$CoFe_2O_4/H_2O$ flow behavior subjected to different factors/physical parameters over a shrinking disk. To simplify and transform the PDEs, a similarity transformation is applied, resulting in a set of ODEs. The steady similarity solutions are numerically computed using the bvp4c program. The numerical solutions are then presented for variables such as velocity, temperature, thermal rate and skin friction coefficient, considering these different factors. In addition to numerical analysis, statistical evaluation is also performed using the RSM. This approach allows for the examination of the relationship between the input parameters and the responses. To summarize the findings, the details of the study's outcomes are as follows:

i. Dual solutions are detected within the specific use of physical factors, however the stable first solution is selected based on the first fulfillment of the far field condition.
ii. For the present problem, the magnetic field, suction parameter and total volumetric concentrations of the hybrid nanoparticles give a significant impact to the skin friction coefficient.
iii. Meanwhile, for the heat transfer rate, only suction parameter significantly affects the heat transfer rate.
iv. Both magnetic and suction parameters enhance the velocity profile while reduce the fluid temperature.
v. However, the present findings are only conclusive to this problem only with the used values of the parameters. There are limitations in choosing the parameters' values.
vi. More investigations are necessary to observe the hybrid nanofluid flow and response surface analysis.

Acknowledgement
The financial support (FRGS/1/2021/STG06/UTEM/03/1 and JURNAL/2020/FTKMP/Q00050) is received from Universiti Teknikal Malaysia Melaka (UTeM) and Ministry of Higher Education (MoHE Malaysia).

References

[1] Crane, Lawrence J. "Flow past a stretching plate." *Zeitschrift für angewandte Mathematik und Physik ZAMP* 21 (1970): 645-647. https://doi.org/10.1007/BF01587695
[2] Miklavčič, M., and C. Wang. "Viscous flow due to a shrinking sheet." *Quarterly of Applied Mathematics* 64, no. 2 (2006): 283-290. https://doi.org/10.1090/S0033-569X-06-01002-5
[3] Wang, C. Y. "Stagnation flow towards a shrinking sheet." *International Journal of Non-Linear Mechanics* 43, no. 5 (2008): 377-382. https://doi.org/10.1016/j.ijnonlinmec.2007.12.021
[4] Sheremet, Mikhail, Dalia Sabina Cimpean, and Ioan Pop. "Thermogravitational convection of hybrid nanofluid in a porous chamber with a central heat-conducting body." *Symmetry* 12, no. 4 (2020): 593. https://doi.org/10.3390/sym12040593
[5] Sheremet, Mikhail, Teodor Grosan, and Ioan Pop. "MHD free convection flow in an inclined square cavity filled with both nanofluids and gyrotactic microorganisms." *International Journal of Numerical Methods for Heat & Fluid Flow* 29, no. 12 (2019): 4642-4659. https://doi.org/10.1108/HFF-03-2019-0264
[6] Sheremet, Mikhail A., Teodor Grosan, and Ioan Pop. "Thermal convection in a chamber filled with a nanosuspension driven by a chemical reaction using Tiwari and Das' model." *International Journal of Numerical Methods for Heat & Fluid Flow* 31, no. 1 (2021): 452-470. https://doi.org/10.1108/HFF-05-2020-0282
[7] Babazadeh, Houman, Mikhail A. Sheremet, Hussein A. Mohammed, Mohammed Reza Hajizadeh, and Zhixiong Li. "Inclusion of nanoparticles in PCM for heat release unit." *Journal of Molecular Liquids* 313 (2020): 113544. https://doi.org/10.1016/j.molliq.2020.113544

[8] Zhang, Xiaojian, M. Sheikholeslami, M. Jafaryar, Mikhail A. Sheremet, Ahmad Shafee, and Houman Babazadeh. "Simulation for melting of paraffin for saving energy with utilize of nanoparticles." *Journal of Molecular Liquids* 313 (2020): 113574. https://doi.org/10.1016/j.molliq.2020.113574

[9] Devi, SP Anjali, and S. Suriya Uma Devi. "Numerical investigation of hydromagnetic hybrid Cu–Al2O3/water nanofluid flow over a permeable stretching sheet with suction." *International Journal of Nonlinear Sciences and Numerical Simulation* 17, no. 5 (2016): 249-257. https://doi.org/10.1515/ijnsns-2016-0037

[10] Devi, S. Suriya Uma, and SP Anjali Devi. "Numerical investigation of three-dimensional hybrid Cu–Al2O3/water nanofl uid flow over a stretching sheet with effecting Lorentz force subject to Newtonian heating." *Canadian Journal of Physics* 94, no. 5 (2016): 490-496. https://doi.org/10.1139/cjp-2015-0799

[11] Bakar, Shahirah Abu, Norihan Md Arifin, and Ioan Pop. "Mixed Convection Hybrid Nanofluid Flow past a Stagnation-Point Region with Variable Viscosity and Second-Order Slip." Journal of Advanced Research in Micro and Nano Engineering 12, no. 1 (2023): 1-21. https://doi.org/10.37934/armne.12.1.121

[12] Takabi, Behrouz, and Saeed Salehi. "Augmentation of the heat transfer performance of a sinusoidal corrugated enclosure by employing hybrid nanofluid." *Advances in Mechanical Engineering* 6 (2014): 147059. https://doi.org/10.1155/2014/147059

[13] Harun, Muhammad Arif, Nor Azwadi Che Sidik, Yutaka Asako, and Tan Lit Ken. "Recent review on preparation method, mixing ratio, and heat transfer application using hybrid nanofluid." *Journal of Advanced Research in Fluid Mechanics and Thermal Sciences* 95, no. 1 (2022): 44-53. https://doi.org/10.37934/arfmts.95.1.4453

[14] Sidik, Nor Azwadi Che, Isa Muhammad Adamu, Muhammad Mahmud Jamil, G. H. R. Kefayati, Rizalman Mamat, and G. Najafi. "Recent progress on hybrid nanofluids in heat transfer applications: a comprehensive review." *International communications in heat and mass Transfer* 78 (2016): 68-79. https://doi.org/10.1016/j.icheatmasstransfer.2016.08.019

[15] Sundar, L. Syam, Korada Viswanatha Sharma, Manoj K. Singh, and A. C. M. Sousa. "Hybrid nanofluids preparation, thermal properties, heat transfer and friction factor–a review." *Renewable and Sustainable Energy Reviews* 68 (2017): 185-198. https://doi.org/10.1016/j.rser.2016.09.108

[16] Shameli, Kamyar, Siti Rahmah Aid, Nur Farhana Arissa Jonny, and Yutaka Asako. "Green Synthesis of Gold Nanoparticles Based on Plant Extract for Nanofluid-based Hybrid Photovoltaic System Application." Journal of Research in Nanoscience and Nanotechnology 4, no. 1 (2021): 19-34.

[17] Idris, Muhammad Syafiq, Irnie Azlin Zakaria, and Wan Azmi Wan Hamzah. "Heat transfer and pressure drop of water based hybrid Al2O3: SiO2 nanofluids in cooling plate of PEMFC." *Journal of Advanced Research in Numerical Heat Transfer* 4, no. 1 (2021): 1-13. https://doi.org/10.37934/arfmts.88.3.96109

[18] Waini, Iskandar, Anuar Ishak, and Ioan Pop. "Unsteady flow and heat transfer past a stretching/shrinking sheet in a hybrid nanofluid." *International Journal of Heat and Mass Transfer* 136 (2019): 288-297. https://doi.org/10.1016/j.ijheatmasstransfer.2019.02.101

[19] Waini, Iskandar, Anuar Ishak, and Ioan Pop. "Unsteady hybrid nanofluid flow on a stagnation point of a permeable rigid surface." *ZAMM-Journal of Applied Mathematics and Mechanics/Zeitschrift für Angewandte Mathematik und Mechanik* 101, no. 6 (2021): e202000193. https://doi.org/10.1002/zamm.202000193

[20] Zainal, Nurul Amira, Roslinda Nazar, Kohilavani Naganthran, and Ioan Pop. "Unsteady stagnation point flow of hybrid nanofluid past a convectively heated stretching/shrinking sheet with velocity slip." *Mathematics* 8, no. 10 (2020): 1649. https://doi.org/10.3390/math8101649

[21] Zainal, Nurul Amira, Roslinda Nazar, Kohilavani Naganthran, and Ioan Pop. "Unsteady three-dimensional MHD non-axisymmetric Homann stagnation point flow of a hybrid nanofluid with stability analysis." *Mathematics* 8, no. 5 (2020): 784. https://doi.org/10.3390/math8050784

[22] Khashi'ie, Najiyah Safwa, Norihan M. Arifin, and Ioan Pop. "Unsteady axisymmetric flow and heat transfer of a hybrid nanofluid over a permeable stretching/shrinking disc." *International Journal of Numerical Methods for Heat & Fluid Flow* 31, no. 6 (2021): 2005-2021. https://doi.org/10.1108/HFF-07-2020-0421

[23] Mehmood, Tahir, Muhammad Ramzan, Fares Howari, Seifedine Kadry, and Yu-Ming Chu. "Application of response surface methodology on the nanofluid flow over a rotating disk with autocatalytic chemical reaction and entropy generation optimization." *Scientific Reports* 11, no. 1 (2021): 4021. https://doi.org/10.1038/s41598-021-81755-x

[24] Mahanthesh, B., and K. Thriveni. "Nanoparticle aggregation effects on radiative heat transport of nanoliquid over a vertical cylinder with sensitivity analysis." *Applied Mathematics and Mechanics* 42 (2021): 331-346. https://doi.org/10.1007/s10483-021-2687-7

[25] Vahedi, Seyed Masoud, A. Zare Ghadi, and Mohammad Sadegh Valipour. "Application of response surface methodology in the optimization of magneto-hydrodynamic flow around and through a porous circular cylinder." *Journal of Mechanics* 34, no. 5 (2018): 695-710. https://doi.org/10.1017/jmech.2018.1

[26] Abdelmalek, Zahra, B. Mahanthesh, Md Faisal Md Basir, Maria Imtiaz, Joby Mackolil, Noor Saeed Khan, Hossam A. Nabwey, and I. Tlili. "Mixed radiated magneto Casson fluid flow with Arrhenius activation energy and Newtonian

heating effects: Flow and sensitivity analysis." *Alexandria Engineering Journal* 59, no. 5 (2020): 3991-4011. https://doi.org/10.1016/j.aej.2020.07.006

[27] Waini, Iskandar, Najiyah Safwa Khashi'ie, Abdul Rahman Mohd Kasim, Nurul Amira Zainal, Khairum Bin Hamzah, Norihan Md Arifin, and Ioan Pop. "Unsteady magnetohydrodynamics (MHD) flow of hybrid ferrofluid due to a rotating disk." *Mathematics* 10, no. 10 (2022): 1658. https://doi.org/10.3390/math10101658